Pergamon

Tetrahedron: Asymmetry, Vol. 8, No. 8, pp. 1207–1224, 1997

Printed in Great Britain
PII: S0957-4166(97)00108-0
0957-4166/97 $17.00 + 0.00

Synthesis and conformational analysis of a lipotetrasaccharide related to the nodulation factor of *Rhizobium* bacteria †

Inmaculada Robina,[a,*] Eugenia López-Barba,[a] Jesús Jiménez-Barbero,[b] Manuel Martín-Pastor[b] and José Fuentes[a]

[a] Departamento de Química Orgánica, Facultad de Química, Universidad de Sevilla, Apartado, 553, E-41071 Sevilla, Spain

[b] Grupo de Carbohidratos, Instituto de Química Orgánica, Juan de la Cierva 3, E-28006, Madrid, Spain

Abstract: The synthesis of the lipotetrasaccharide glycoside, *p*-methoxyphenyl O-{2-deoxy-2-[(11Z)-11-octadecenoylamido]-β-D-glucopyranosyl}-(1→4)-*O*-(β-D-glucopyranosyl)-(1→4)-*O*-β-D-glucopyranosyl)-(1→4)-2-acetamido-2-deoxy-β-D-glucopyranoside **16**, starting from acetobromocellobiose is reported. Compound **16** is an analogue of the nodulation factors of *Rhizobium* bacteria having the central chitobiose unit substituted by a cellobiose unit. A conformational study indicates that **16** have restricted fluctuations around the glycosidic torsion angles, but can adopt a variety of shapes. © 1997 Elsevier Science Ltd

Introduction

The leguminous plants and their specific symbiotic bacteria of the genus *Rhizobium* are responsible for the assimilation of atmospheric nitrogen by plants. In the symbiosis, at an early stage of the infection process, the bacteria provoke the formation of particular organs, the nodules, in which they reduce molecular nitrogen to ammonia and in this way, it is assimilated by the plants.[1] The symbiosis is specific: one type of *Rhizobium* infects one type of leguminous plant, and both partners exchange low molecular-weight signal molecules. The plants control the bacteria by secreting flavonoids and the *Rhizobia* respond to plants by synthesising specific extracellular signal molecules named LCOs or *Nod*-factors. These *Nod*-factors have been shown to be in all cases lipooligosaccharides comprising a tetra- or pentasaccharidic backbone of chitin bearing several substituents at both ends. Thus for instance, the LCO secreted by *Rhizobium meliloti*[2] is a lipotetrasaccharide of *N*-acetyl-D-glucosamine with a sulfate group on the C-6 position of the reducing-end. The LCO synthetized by *Rhizobium leguminosarum*[3] has in the non-reducing end an acetate group on the carbon-6. The molecule secreted by *Bradyrhizobium japonicum*[4] is a tetra- or pentasaccharide and has a 2-*O*-methylfucose sugar α-glycosylated at the carbon-6 of the reducing end. The *Nod*-factor secreted by *Rhizobium fredii*[5] is a tri-, tetra- or pentasaccharide which has a fucose or 2-*O*-methylfucose α-glycosylated on the carbon-6 of the reducing end. In all the cases there is a fatty *N*-acyl group on the non-reducing aminosugar end. These fatty acyl moieties are C16 or C18 chains which contain one, two, three or four double bonds. There is a *cis*-double bond located between C9 and C10 or between C11 and C12 whereas the other double bonds are *trans*-conjugated to the carbonyl group.

The important role of these molecules in the study of the signal-exchange process and host specificity, and the scarcity of their natural occurrence has encouraged several groups to perform their chemical synthesis. In the last five years several strategies to obtain LCOs have been developed.[6–10]

With the aim of finding smaller fragments of the molecule still possessing biological activity or for studying their potential activity, the synthesis of related molecules to *Nod* factors is reported. Among

† Dedicated to Professor H. Paulsen on the occasion of his 75th birthday.

* Corresponding author. Email: robina@cica.es

these molecules are trisaccharide[11] and thio-trisaccharide analogues,[12] chitin oligosaccharides,[13] and branched oligosaccharides.[14]

At the same time glycolipids have been described as immunomodulators.[15] Recently, vaccines have been developed using as antigen refined surface structures of pathogens which, to elicit the protective effect, frequently need the simultaneous use of adjuvants.[16] Among these adjuvants are several classes of conjugates of carbohydrates and lipids, which have an amino mono- or oligosaccharide (aminosugar and glycosylamine) as glycosyl moiety and one or several fatty acyl chains frequently on the amino group. The best compounds for biological studies[15] are those containing non protected sugar units due to their water solubility.

Biological and chemical properties of organic compounds strongly depend on their configuration and conformation. The amide *Z/E* isomerism due to hindered rotation about the C–N bond has been studied in sugar amido derivatives[11,17,18] and the *EZ*⇌*ZZ* equilibrium has been proposed as major configurations for chloroformic solutions of an *O*-acetylated *N*-acyltrisaccharide.[11] As far as we are aware the molecular dynamic calculations and the ROESY NMR experiments have not been applied to study the total stereochemistry of *O*-unprotected *N*-acylamino-oligosaccharides.

Only very small concentrations (10^{-6}–10^{-12} M) of natural LCO factors are required to initiate nodulation but the activity is limited by the action of chitinases that cleave the oligosaccharides at the glycosidic bond linking the two central units. In order to facilitate studies on the biological importance of the two central acetamido groups, in this paper we describe the synthesis of the unprotected lipotetrasaccharide **16**, and of the protected analogues **12–15** and **17**. These structures are related to those of rhizobia LCOs[1] and glycolipid immunomodulators.[15] The chitobiose central unit of LCOs has been changed by a cellobiose moiety. With this change we expect a major resistance to the chitinase action. The synthetic strategy involves two *O*-glycosylations using the thioglycoside and the trichloroacetimidate methods.[19] The conformational analysis of **16** has been performed using simulation and molecular dynamic programmes and also inter-residue N.O.E. experiments.

Results and discussion

For the synthesis of the lipooligosaccharide **16** we have to bear in mind its size, with four sugar units, the variety of its functional groups and the stereochemistry of the glycosidic bonds. The general retrosynthetic analysis is outlined in Scheme 1.

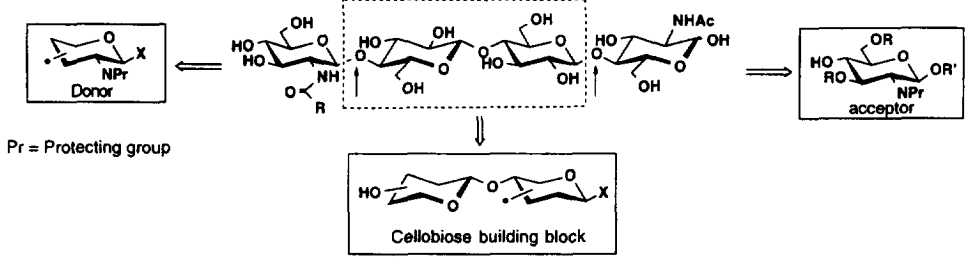

Scheme 1. Retrosynthetic analysis of **16**.

Using cellobiose as building block, the key steps in the retrosynthetic analysis are two disconnections involving each one β(1→4) glycosylations reactions, that led to a glycosyl donor and a glycosyl acceptor derived from D-glucosamine, each of them will have to join to a suitable protected cellobiose building block. The construction of properly substituted derivatives of mono and oligosaccharides is of critical importance for the stereoselective couplings, for the regioselective amidation with the fatty acyl chain, and deprotection without touching the unsaturated double bond of the lipid moiety. With respect to the protecting groups we have chosen the OMP (*p*-methoxyphenyl group) for the anomeric position because it gives a high degree of flexibility to the total synthesis: it can be removed under

conditions that do not affect neither the glycosidic bonds nor other functional groups present in the molecule and is also stable under the wide range of reaction conditions necessary for hydrogenolysis, hydrazinolysis, and also is resistant to the action of the Lewis acids used in benzylidenation and glycosylation reactions. Other groups employed to protect the anomeric positions such as allyl (OAll), *tert*-butyldimethylsilyl (OTBDMS), benzyl, etc., would not have resisted those kinds of reaction conditions.

With respect to the synthons derived from D-glucosamine to achieve a high-yielding glycosylation reaction, the choice of the protecting groups is important: thus the nitrogen-protecting group not only is interesting in the donor as a way of controlling the stereochemistry, but also in the acceptor as a way of increasing its reactivity.

To achieve the synthetic sequence of **16** the first reaction is the coupling of the synthons **1** and **2**[20] (Scheme 2). The HO-4 group of compound **2** is very unreactive,[21] especially when the ring is in the $^4C_1$ conformation. This low reactivity demands a careful choice of the protecting groups of the amino and hydroxy functions that in general, should not be electron-withdrawing. *N*-Phthaloyl group is an obvious choice as a temporary protecting group for nitrogen because of the high yield observed in the β(1→4) glycosylation with a low-activated HO-4 glucosamine acceptor.[22,23] With respect to the protection of the hydroxy groups, on the positions C-3 and C-6, benzyl groups have proved[24] to be highly suitable regarding to increase the yield of the glycosylation method. Other groups such as bulky groups or electron-withdrawing groups are not efficient because they do not improve the known low reactivity of the HO-4 group in glucosamine and derivatives.

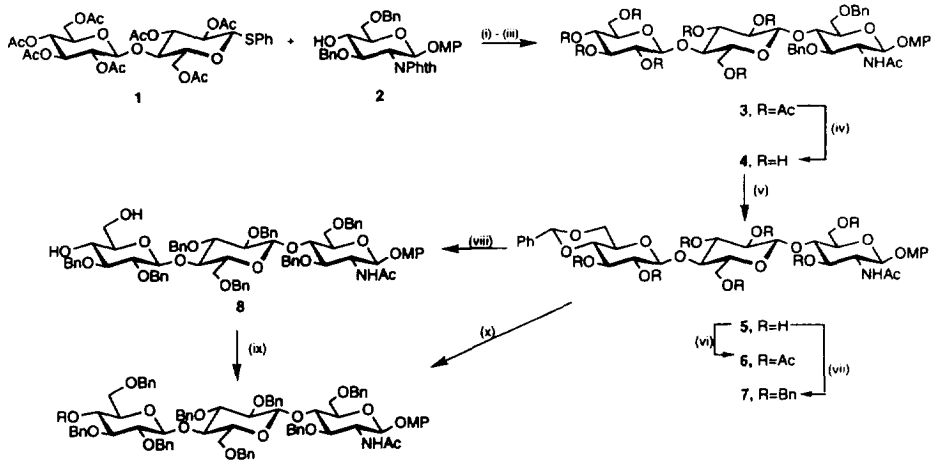

Reagents and conditions:
(i) NIS/TfOH, Cl_2CH_2; (ii)$N_2H_4.H_2O$, EtOH; (iii) Ac_2O/py; Yield (i+ii+iii)=80%
(iv) MeONa/MeOH; (v) PhCHO, $ZnCl_2$; Yield (iv +v)=90%
(vi) Ac_2O/py; Yield=91% ; (vii) BrBn, NaOH, Bu_4NHSO_4, DMF, Bu^tOH; Yield=60%
(viii) PTSA, Cl_2CH_2; Yield=55%; (ix) BrBn, Bu_2SnO, Bu_4NBr, MeCN; Yield=80%
(x) $NaCNBH_3$, HCl/ether, THF; Yield=60%; (xi) Ac_2O/py; Yield=95%

Scheme 2.

The second part of the synthesis of **16** is outlined in Scheme 3. To have stereocontrol in the glycosylation reaction[25] we have chosen as participating group at C-2 the phthalimido in compound **11** and the acetate in the thioglycoside **1**. On the other hand, the presence in **16** of two differently substituted amino fuctions requires the transformation of one phthalimido group into the acetamido just before the second glycosylation reaction. Finally, it is worth pointing out that the insaturation in the fatty chain requires the elimination of the benzyl groups before the introduction of the lipid moiety.

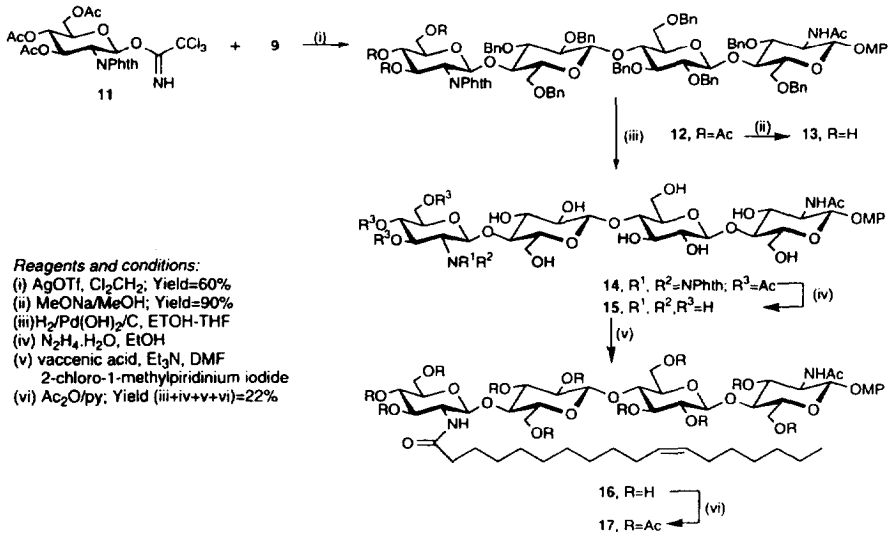

Scheme 3.

The known[26] phenyl heptaacetyl β-cellobioside **1** was obtained in 60% yield by reaction of acetobromocellobiose and thiophenol under phase transfer catalysis conditions. The reaction of **1** and **2** in the presence of *N*-iodosuccinimide and a catalytic amount of triflic acid[27] afforded, with quantitative β-stereoselectivity, the corresponding trisaccharide that, after hydrazinolysis and acetylation gave the trisaccharide **3** in 80% yield. Zemplén deacetylation of **3** followed by benzylidenation with benzaldehyde and zinc chloride afforded **5** in 90% overall yield, which was characterized as its acetate **6**. Subsequent treatment of **5** with benzyl bromide under phase transfer catalysis[11,20,28] gave **7** in 60% yield. From this compound the preparation of **9** was performed following two pathways: *a*, cleavage of the benzylidene acetal that renders the diol **8** in 55% yield followed by regioselective benzylation (80% yield) *via* tin-derivatives of the resultant diol; *b*, regioselective reduction with sodium cyanoborohydride that gave **9** directly in 60% yield.

For the glycosylation of **9** we chose the trichloroacetimidate–silver triflate method.[29–31] The reaction of the glycosyl acceptor **9** with the imidate **11** in the presence of AgOTf in dichloromethane afforded with quantitative β-stereoselectivity (as expected from the directing effect of the phthalimido group) the tetrasaccharide **12** in 60% yield. Hydrogenolysis in the presence of $Pd(OH)_2$ followed by treatment with hydrazine in ethanol under reflux gave the aminotetrasaccharide **15** which was not isolated. *N*-Acylation of **15** with vaccenic acid in the presence of 2-chloro-1-methyl-pyridinium iodide[32] gave the *O*-unprotected tetrasaccharide **16** derivative in 22% overall yield (NMR data, Table 2). Subsequent acetylation produced the lipooligosaccharide glycoside **17** in 90% yield.

The structures of compounds **3–9** and **12–17** are supported by analytical, NMR[33] (Tables 1 and 2 and Experimental) and MS spectroscopic data. In the case of compound **9** the acetyl derivative **10** was prepared to confirm the position of the hydroxyl group. The resonance of H-1′ (4.51 ppm, $J_{1',2'}$=8.1 Hz) in **3** confirms the β-stereoselectivity of the glycosylation reaction. The chemical shift of the resonance of H-4′ in **10** was ≈ 4.95 ppm showing a downfield shift with respect to the same signal in **9** as corresponds to the acetylation. For compound **12** the resonance of H-1‴ (5.51 ppm, $J_{1''',2'''}$=8.3 Hz) confirms the β-stereoselectivity of the glycosylation reaction. In addition, the resonances of H-1‴ and H-3‴ of compound **12** showed the described[34] deshielding influence of an equatorial diacylamino group on the adjacent axial protons. Nevertheless a shielding effect (≈ 5 ppm)[11] was observed in the resonance of C-1‴.

In the case of compound **16**, a conformational analysis (Figure 1) was performed using different

Table 1. Selected NMR data (δ, ppm; *J*, Hz) of compounds **3**, **6**, **9**, **10**, **12**, **17**

Comp.	H-1	H-1'	H-1"	H-1"'	$J_{1,2}$	$J_{1',2'}$	$J_{1",2"}$	$J_{1"',2"'}$	C-1	C-1'	C-1"	C-1"'
3[a]	5.26d	4.51d	4.44d	-	5.7	8.1	8.1	-	98.6	99.2	100.6	-
6[b]	5.16d	4.45d	4.46d	-	9.5	8.5	8.0	-	98.6	99.2	101.5	-
9[a]	5.38d	4.52-4.48m	4.52-4.48m	-	6.8	-	-	-	98.7	102.3	102.9	-
10[b]	5.31d	4.81-4.33m	4.81-4.33m	-	6.9	-	-	-	98.9	102.1	102.9	-
12[a]	5.33d	4.40-4.16m	4.40-4.16m	5.51d	6.7	-	-	8.3	97.7	101.1	102.3	95,4
17[a]	4.96d	4.56-4.42m	4.56-4.42m	4.56-4.42m	7.1	-	-	-	99.8	100.2	100.6	100.8

[a] In $CDCl_3$, 500 MHz (^1H), 125.7 MHz (^{13}C); [b] In $CDCl_3$, 500 MHz (^1H), 75.4 MHz (^{13}C);
[c] Peaks that may be interchangeable.

Table 2. NMR data (δ, ppm) of compound **16** in methanol-d_4

Ring	H-1	H-2	H-3	H-4	H-5	H-6a	H-6b	NH	OMe	AcN	HO-2	HO-3	HO-4	HO-6	Arom	CH=CH
A	4.87	3.69	3.43	3.42	3.58	3.42	3.76	7.86	3.70	1.81		4.64	-	4.58	6.85 6.92	4.58
B(')	4.35	3.06	3.54	3.26	3.50	3.57	3.80	-	-	-	4.63	4.62	-	4.67		4.67
C(")	4.30	3.04	3.29	3.26	3.42	3.40	3.62	-	-	-	4.63	4.67	-	4.76		4.76
D(")	4.37	3.44	3.26	3.06	3.18	3.45	3.75	2.06	-	-	-	4.89	5.03	4.69		4.69

	C-1	C-2	C-3	C-4	C-5	C-6	OMe	AcN	Arom
A	100.6	55.5	73.2	69.2	72.4	61.5	58.0	23.1	114.8
B(')	102.2	73.6	74.5	81.0	74.8	60.5			
C(")	101.0	73.6	74.5	81.0	75.0	60.4			
D(")	103.4	55.3	72.8	70.5	76.5	59.5		35.8	

approaches. First, a *Monte Carlo* (MC) approach was chosen which produced 354 different conformers. However, only three of them presented steric energies under 12 KJ.mol^{-1} over the obtained global minimum. Thus, only these three structures were deeply analysed. A view of the geometries of these minima is given in Figure 2. The glycosidic torsion angles φ/ψ found for the global minimum (Min. 1) are *ca.* (60°/0°), are typical for β(1→4) linked disaccharides,[35] also in agreement with the operativity of the exo-anomeric effect. The other two minima obtained (Min. 2 and Min. 3) present deviations from these values for only one of the three φ/ψ torsions.

In fact, for Min. 2, the glycosidic torsions φ2/ψ2 are 37/−49°, respectively, while for Min. 3, similar values are found for torsion φ1/ψ1 (34/59°). These angles also correspond to one local minimum within the lowest energy region of the φ/ψ potential energy map of β(1→4) linked disaccharides. Inspection of the corresponding geometry allows to deduce that this deviation from normal values is induced by the formation of an inter-residue hydrogen bond between O3 of the glycosidic sugar and O6 of the following aglyconic residue, with the corresponding hydroxymethyl group in the stable *gt* conformation. The geometry allows that either O3′ or O6 oxygens may act as both H-bond donor or acceptor.

The conformational space around the global minimum, Min. 1, was extensively scanned and fifteen additional related conformations were generated (Figure 2). In particular, *gg* and *gt* rotamers were combined for the four hydroxymethyl torsions of the different residues, namely, ω1, ω2, ω3 and ω4. The rest of the oligosaccharide structure was kept fixed. Subsequent minimization of these starting

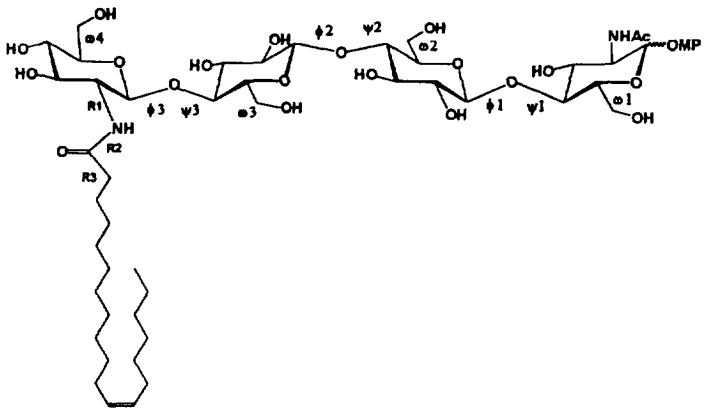

Figure 1. Glycosidic torsion angles of **16**.

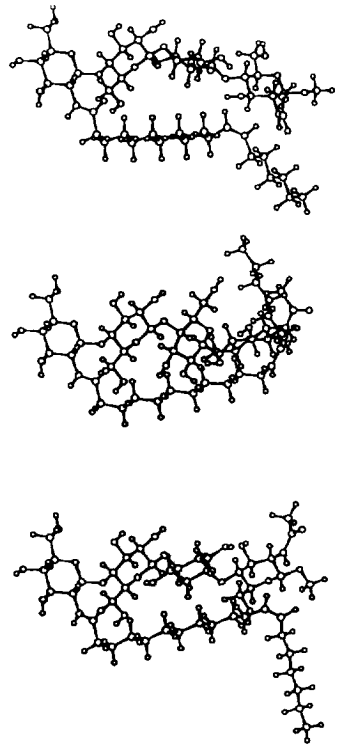

Figure 2. Schematic view of the local minima of compound **16** as calculated by MM3*.

conformations did not affect the glycosidic torsion values, which remained fairly similar to those described for Min. 1. The lowest energy conformation is that with an all *gt* orientation (ω *ca.* 60°), which indeed corresponds that previously generated (Min. 1). Nevertheless, the rest of possibilities also have to be taken into account since the steric energy differences found among these minima are fairly small, in fact, less than 6 KJ.mol^{-1}, which may indicate that all the fifteen conformations may have a certain population at room temperature.

The relevant interatomic distances are shown in Table 3. Min. 2 presents an O3 (residue 2)–O6 (residue 3) of 3.0 Å, while Min. 3 presents an O3 (residue 1)–O6 (residue 2) of 3.2 Å, corresponding

Table 3. Relevant interatomic distances for the minima of compound **16**, as found by molecular mechanic and dynamic calculations

Proton Pair	Min.1	Min.2	Min.3	MD-MM3* $\langle r\text{-}6\rangle^{-1/6} - \langle r\text{-}3\rangle^{-1/3}$	MD-CVFF $\langle r\text{-}6\rangle^{-1/6} - \langle r\text{-}3\rangle^{-1/3}$
H-1 res*2* – H-4 res*1*	2.35	2.37	2.44	2.38 – 2.40	2.24 – 2.24
H-1 res*2* – H-6a res*1*	3.23	3.24	4.54	4.23 – 4.30	3.73 – 3.82
H-1 res*2* – H-6b res*1*	2.72	2.72	4.12	2.68 – 2.82	3.46 – 3.62
H-1 res*3* – H-4 res*2*	2.37	2.33	2.30	2.36 – 2.38	2.22 – 2.23
H-1 res*3* – H-6a res*2*	2.76	4.27	3.23	3.23 – 3.59	3.81 – 3.85
H-1 res*3* – H-6b res*2*	2.36	3.91	2.30	2.86 – 3.04	3.59 – 3.67
H-1 res*4* – H-4 res*3*	2.56	2.43	2.49	2.40 – 2.43	2.43 – 2.43
H-1 res*4* – H-6a res*3*	3.01	3.01	2.97	3.43 – 3.72	4.56 – 4.56
H-1 res*4* – H-6b res*3*	2.42	2.41	2.43	2.84 – 3.13	4.32 – 4.32
O-3 res*1* – O-5 res*2*	2.70	2.70	2.77	2.79 – 2.83	2.94 – 2.95
O-3 res*2* – O-5 res*3*	3.12	2.66	2.75	2.80 – 2.83	2.91 – 2.91
O-3 res*3* – O-5 res*4*	3.04	2.99	2.96	3.14 – 3.28	3.66 – 3.67
O-3 res*1* – O-6res*2*	3.58	3.63	3.21	3.93 – 4.05	3.67 – 3.69
O-3 res*2* – O-6 res*3*	4.06	3.06	3.50	4.07 – 4.26	3.53 – 3.55
O-3 res*3* – O-6 res*4*	4.27	4.11	4.18	4.53 – 4.69	3.60 – 3.62

res *1* corresponds to ringA, res *2* to ring B, res *3* to ring C, and res *4* to ring D.

to hydrogen bond contacts. In order to check the influence of this H-bond in the glycosidic torsion values, the three conformers, Min. 1, 2 and 3 were further minimized using MM3*, now using the GB/SA solvent[36] model for water, instead of a bulk dielectric constant. No important changes in the structural features were found, although the calculated steric energies now pointed to a new global minimum, Min. 2. Therefore, this MC/MM approach points to the existence of certain degree of flexibility around the glycosidic linkages of **16**.

In a second step, the conformational stability of the global minimum of **16** was studied through *molecular dynamics* simulations.[37] Two independent (MD-I and MD-II) simulations were performed, as described in the Experimental section. The first simulation, MD-I, was performed by using the MM3* force field as described in the Experimental section, using the global minimum (Min. 1) as starting structure. The Φ/Ψ trajectories are depicted in Figure 3. It can be observed that, during the simulation, the glycosidic torsion angles remained most of the time around their original values close to the global minimum, with no transitions to other regions of the map, thus confirming the stability of this conformer. On the other hand, the hydroxymethyl group torsions underwent frequent transitions from *gt* to *gg* orientations, thus confirming the low energy barrier which separates both conformations, easily accessible at room temperature. Some excursions to the *tg* region were also observed.

A superimposition of five structures, taken at 100 ps intervals of MD-I, is depicted in Figure 4. Residue 4 of the different frames has been used as reference points, and the figure shows that, despite the relatively narrow variation of the glycosidic torsion angles, the conformational space accesible to the tetrasaccharide and to the lipid chain may be fairly large.

A second MD simulation, MD-II, was performed by using a different force field. In this case, the CVFF programme[38] was employed, as described in the Experimental section, and the global minimum Min. 1 was also used as input geometry. History and trajectory plots are shown in Figure 5. It can be observed (Figure 5) that the CVFF trajectory was stabilized 125 ps. The glycosidic torsion angles remained most of the time close to those of the global minimum. The trajectories of the four hydroxymethyl groups showed several interconversions during the first 20 ps of the simulation, and then, all of them adopted the *gt* orientation, except $\omega 4$, which changed to the *tg* rotamer.

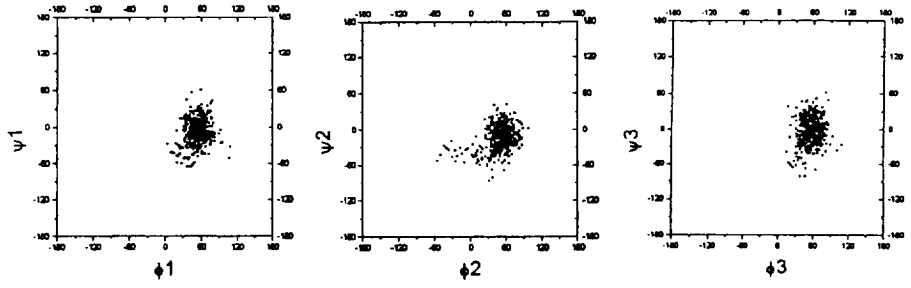

Figure 3. Trajectory plots of the different glycosidic linkages of **16** in Φ/Ψ spaces, as calculated by MD simulations using MM3* programme.

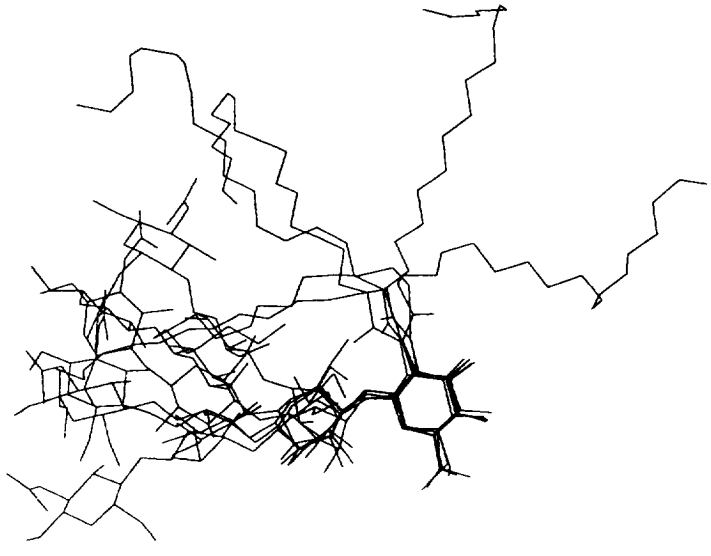

Figure 4. Superimposition of five snapshots taken during the MD-MM3* simulation of compound **16**. The non-reducing end pyranoid ring was chosen for the superimposition. The accesible conformational space may be appreciated.

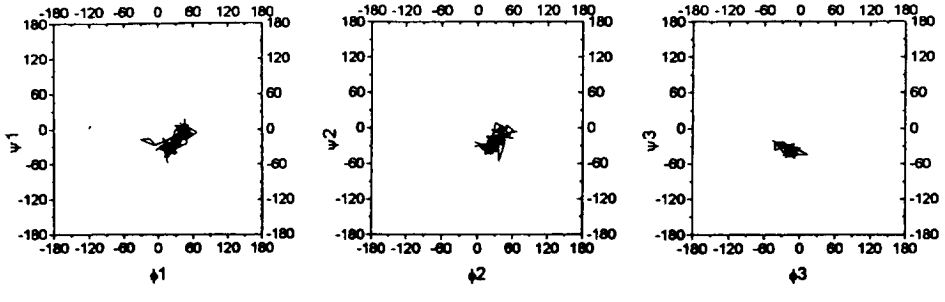

Figure 5. Trajectory and history plots of Φ and Ψ angles of the different glycosidic linkages of **16** calculated by MD simulation using the CVFF programme.

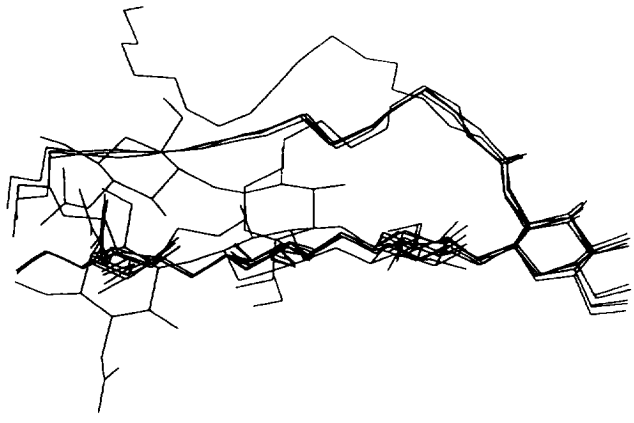

Figure 6. Superimposition of five snapshots taken during the MD-CVFF simulation of compound **16**. The non-reducing end pyranoid ring was chosen for the superimposition. The accesible conformational space may be appreciated.

A superimposition of five structures taken also at 100 ps intervals during MD-II is presented in Figure 6. In this case, the accessible conformational space to the tetrasaccharide seems also to be smaller than that predicted by simulation MD-I. This conclusion is evident not only from the comparison of Figs 4 and 5, but also from the dispersion of values found in the two sets of Φ/Ψ plots (Figs 3 and 5). Nevertheless, both force fields are in agreement with the unique presence of conformers within the central region of the maps. Interoxygen O3′–O5 distances are indicative of the possible presence of hydrogen bonds (Table 3). The corresponding average distances found during MD-I (MM3*) allowed to deduce that the three possible hydrogen bonds of these type are likely to be present during most of the simulation time. In contrast, during MD-II (CVFF), the corresponding average distances indicated that only two of them were possible. The corresponding interoxygen distance between those atoms in residues 3 and 4 is too high.

Regarding the orientation of the lipid chain, it can be observed that the MC search produced a geometry which is very similar for all the minima (Figure 2). According to the calculations, the aliphatic chain adopts a quasi-parallel disposition with regard to the tetrasaccharide, thus making van der Waals contacts below 3.7 Å, with the hydrophobic patch of the sugar units. This disposition indeed favors the stabilization by means of hydrophobic interactions. In fact, during simulation MD-II, the lipid chain showed a very limited range of motion (Figure 6), and remained in close contact with the sugar residues, as also found in the global minimum geometry. In contrast, simulation MD-I predicted a higher range of flexibility of the lipid chain with respect to the sugar moieties, as can be seen in Figure 4.

NMR results on **16**. The first step was the assignment of the different ^{1}H and ^{13}C NMR resonances of **16** through a combination of ROESY, TOCSY, and HMQC techniques.[39] The corresponding data are shown in Table 2. Several reports,[35] for β(1→4) linked disaccharides, have presented the existence of inter-residue NOE contacts between the anomeric proton and H-4 of the contiguous aglyconic-type sugar, as well as the presence of NOEs between the anomeric proton and the H-6′s in the same aglyconic moiety. These NOEs are exclusive of ϕ/ψ conformations within the main region of the energy map, like those described above in the present paper for the glycosidic torsions of minima 1, 2, and 3, as well as for most of the time of both MD-I and MD-II simulations. Nevertheless, the presence of these inter-residue NOEs for **16**, is rather difficult to assure experimentally because of the extensive overlapping of H-4 and H-3 resonances in the ^{1}H NMR spectra. On the other hand, the H-1′/H-6 NOEs are clearly observed in the ROESY spectra.

In order to evaluate, at least qualitatively, the validity of the MC and MD structures obtained during the calculations, the following simplified analysis, which considered the experimental NOE contacts,[40]

Table 4. Unambiguous experimental ROE contacts and corresponding calculated distances for interresidue proton–proton pairs of compounds **16**

Experimental ROESY cross peak	Min. 1	Min. 2	Min. 3	MD - MM3* $\langle r\text{-}6\rangle^{-1/6} - \langle r\text{-}3\rangle^{-1/3}$	MD – CVFF $\langle r\text{-}6\rangle^{-1/6} - \langle r\text{-}3\rangle^{-1/3}$
H-1 res*3* – H-6a res*2*	2.76	4.27	3.23	3.23 – 3.59	3.81 – 3.85
H-1 res*3* – H-6bres*2*	2.36	3.91	2.30	2.86 – 3.04	3.59 – 3.67
H-1 res*2* – H-6b res*1*	2.72	2.72	4.12	2.68 – 2.82	3.46 – 3.62
NH res*4* – H-6b res*3*	3.62	3.18	3.16	3.42 – 3.78	2.66 – 2.68
H-1 res*3* – HO-2 res*3*	2.96	2.98	2.96	3.14 – 3.22	2.41 – 2.45
H-1 res*2* – HO-2 res*2*	2.93	2.94	2.94	3.36 – 3.40	2.37 – 2.38
H-1 res*4* – HO-6 res*3*	4.53	2.94	5.15	3.48 – 3.69	6.19 – 6.19

In addition cross peaks for the H-1' – H-4 proton pairs of every glycosidic linkage may be found although they are overlapping with other signals.

was employed.[39] Intense, medium and weak cross peaks should be observed for interproton distances smaller than 2.5, 3.0, and 3.5 Å, respectively. Longer distances would give null cross peaks. The distances shown in Table 3 indicate that all the individual minima (Min. 1 to 3) and the ensemble average calculated from MD-I and MD-II would produce H-1′/H-4 distances smaller than 3 Å and, therefore, intense to medium NOE cross peaks should be observed. As mentioned above, although cross peaks to H-1′ indeed exist at the chemical shift position of all H-4 protons, the overlapping problem makes ambiguous their assignment. On the other hand, unambiguous assignments were obtained for the cross peaks gathered in Table 4. Thus, the experimental H-1 (residue 3)–H-6a,b (residue 2) and H-1 (residue 2)–H-6b (residue 1) are well predicted by the simulations, despite the interconversions observed for the hydroxymethyl groups. In addition, minimum 1, considered as a single conformer, with all the hydroxymethyl groups in the *gt* orientation also explains the presence of these three cross peaks. On the other hand, the exclusive presence of either minimum 2 or minimum 3, as well as the ensemble average distribution obtained from MD-II, only produced partial agreement with the experimental data. Only one experimental cross peak, namely NH (residue 4)–H-6b produced information about the disposition of the lipid chain. Since the interproton distance found for both minimum 1 and for MD-I is about 3.5 Å, this contact is better explained by the presence of minima 2 and/or 3 and by MD-II. One additional inter-residue cross peak, namely H1 (residue 4)–HO6 (residue 3) was also found experimentally. This NOE is rather dependent on the torsion ω3 value and, indeed, it is only compatible with a major *gg* conformation of the corresponding hydroxymethyl moiety. Only MD-I satisfactorily reproduces this observation.

In conclusion, the experimental ROESY cross peaks are satisfactorily explained by MD-I (MM3*/GB-SA solvent model)[36] simulation, although a major conformer (Min. 1) with smaller contributions of minima 2 and/or 3 also produced a good concordance with most of the experimental cross peaks. Therefore, compound **16** seems to have restricted fluctuations around the glycosidic torsion angles, although these oscillations are limited to a fairly narrow of the energy surfaces. Nevertheless, the presence of three contiguous linkages make possible that the tetrasaccharide may adopt a variety of shapes,[41] as those shown in Figure 4.

Experimental

General

Melting points are uncorrected. Optical rotations were measured at 22±1° for solutions in dichloromethane or chloroform. ^{1}H NMR spectra (300 and 500 MHz) were obtained for solutions in $CDCl_3$ or MeOH-d_4, *J* values are given in Hz. In the case of **16** the spectra were measured at 30°C, using a *ca.* 10 mM sample, carefully degassed and sealed under argon. Assignments were confirmed by decoupling, H-D exchange, and homonuclear 2D COSY correlated experiments. The 2D rotating

frame NOE (ROESY, CAMELSPIN) experiments were recorded with a total mixing time was of 300 ms. The RF carrier was set at δ 6.0 ppm to minimize spurious Hartmann–Hahn effects. Selective 1D-ROESY experiments were also performed. Spin locking times of 300 ms were used after inversion of the desired proton with a top-hat selective pulse. ^{13}C NMR spectra were recorded at 75.4, and 125.7 MHz. Heteronuclear 2D correlated spectra were obtained in order to assist in carbon resonance assignments. The pure absorption one bond proton–carbon correlation experiments were collected in the ^{1}H-detection mode using a HMQC pulse sequence and a reverse probe. A relaxation delay of 1 s and a delay corresponding to a J value of 150 Hz were used. A BIRD-pulse was used to minimize the signals arising from protons bonded to ^{12}C. EI-Mass spectra (70 eV) were measured with a KRATOS MS-80RFA instrument, with an ionising current or 100 μA, an accelerating voltage of 4 kV, and a resolution of 1000 (10% valley definition). The FABMS spectra were measured with the same instrument. Ions were produced by a beam of xenon atoms (6–7 KeV) using a matrix consisting of glycerol or thioglycerol and NaI as salt, $(CsI)_{37}Cs$ was used as reference. TLC was performed on Silica Gel HF_{254} (Merck), with detection by UV light or charring with H_2SO_4. Silica Gel 60 (Merck, 230 mesh) was used for preparative chromatography.

Phenyl 2,3,6,2′,3′,4′,6′-hepta-O-acetyl-1-thio-β-cellobioside ***1***

This compound was prepared by the following modification of the described method.[26] A mixture of NaOH (1.42 g, 35.4 mmol) and thiophenol (3.3 mL, 35.4 mmol) in water (8 mL) was stirred for 30 minutes at r.t., then, a solution of acetobromocellobiose (16.70 g, 23.0 mmol) and HSO_4NBu_4 (1.20 g, 4.1 mmol) in dichloromethane (50 mL) was added. The reaction mixture was stirred vigorously for 30 hours and then diluted with dichloromethane. The organic layer was washed with water, dried (Na_2SO_4) and evaporated. Column chromatography of the residue on silica gel (dichloromethane–acetone (30:1→15:1) gave **1** (9.87 g, 60%); FABMS: *m/z* 751 [48%, $(M+Na^+)$].

p-*Methoxyphenyl* O-*(2,3,4,6-tetra-*O*-acetyl-β-D-glucopyranosyl)-(1→4)-*O*-(2,3,6-tri-*O*-acetyl-β-D-glucopyranosyl)-(1→4)-2-acetamido-3,6-di-*O*-benzyl-2-deoxy-β-D-glucopyranoside* ***3***

To a solution of phenyl 2,3,6,2′,3′,4′,6′-hepta-*O*-acetyl-1-thio-β-cellobioside **1** (4.00 g, 5.5 mmol) and *p*-methoxyphenyl 3,6-di-*O*-benzyl-2-deoxy-2-phthalimido-β-D-glucopyranoside **7**[20] (1.64 g, 2.8 mmol) in dry dichloromethane (30 mL) with 4 Å molecular sieves, *N*-iodosuccinimide (2.56 g, 11.8 mmol) under Ar and in the dark, was added. The reaction mixture was stirred at r.t. for 30 minutes and then cooled to 0°C. A solution of TfOH (52 μL) in dichloromethane (45 mL) was added. The reaction mixture was stirred at 0°C for 3 h, diluted with dichloromethane and then filtered through Celite. The solution was washed successively with water, saturated aq $NaHCO_3$, aq $Na_2S_2O_3$ (10%) and water, dried (Na_2SO_4) and evaporated in vacuo. The resultant residue containing *p*-methoxyphenyl *O*-(2,3,4,6-tetra-*O*-acetyl-β-D-glucopyranosyl)-(1→4)-*O*-(2,3,6-tri-*O*-acetyl-β-D-glucopyranosyl)-(1→4)-3,6-di-*O*-benzyl-2-deoxy-2-phthalimido-β-D-glucopyranoside was dissolved in ethanol (420 mL) and $N_2H_4 \cdot H_2O$ (17 mL) was added. The reaction mixture was heated under reflux for 3 days, evaporated in vacuo and coevaporated several times with toluene/ethanol. Pyridine (60 mL) and acetic anhydride (30 mL) were added at 0°C to the residue. After 18 h at r.t. the reaction mixture was poured into ice–water (100 mL) and extracted with dichloromethane (3×40 mL). The organic layer was washed successively with aq H_2SO_4 1 M, saturated aq $NaHCO_3$ and water, dried (Na_2SO_4) and evaporated in vacuo. Column chromatography of the residue on silica gel (dichloromethane–acetone, 20:1→5:1) gave **3** (2.50 g, 80%) as white solid, which crystallised from ethanol had m.p. 164–166°C; $[\alpha]_D$ −28.2 (*c* 1.1, dichloromethane). ^{1}H NMR (500 MHz, $CDCl_3$), Table 1 and δ 7.33–7.26 (m, 10H, Ph), 6.92–6.76 (m, 4H, $C_6H_4OCH_3$), 5.90 (d, 1H, $J_{2,NH}$ 8.2 Hz, N*H*), 5.14–5.04 (m, 3H, H-3′, H-3″, H-4″), 4.93 (t, 1H, $J_{2'',3''}$ 8.1 Hz, H-2″), 4.87 (dd, 1H, $J_{2',3'}$ 9.7 Hz, H-2′), 4.77, 4.65, 4.55, 4.40 (4d, 1H each, $^{2}J_{H,H}$ 11.8, 11.9, 11.9, 11.9 Hz, CH_2Ph), 4.36 (dd, 1H, $J_{5'',6a''}$ 4.2 Hz, $J_{6a,6b}$ 12.7 Hz, H-6″a), 4.05 (dd, 1H, $J_{5',6a'}$ 5.1 Hz, $J_{6a',6b'}$ 12.1 Hz, H-6′a), 4.03–3.99 (m, 2H, H-4, H-6″b), 3.96 (t, 1H, $J_{3,4}$ 6.8 Hz, H-3), 3.91 (ddd, 1H, $J_{2,3}$ 6.8 Hz, H-2), 3.80

(dd, 1H, $J_{5,6a}$ 4.3, $J_{6a,6b}$ 12.4, H-6a), 3.75–3.66 (m, 4H, H-4′, H-5, H-6′b, H-6b), 3.75 (s, 3H, OCH_3), 3.62 (ddd, 1H, $J_{4'',5''}$ 9.7 Hz, $J_{5'',6b''}$ 2.3 Hz, H-5″), 3.35 (ddd, 1H, $J_{4'5'}$ 9.6 Hz, $J_{5',6'a}$ 5.1 Hz, $J_{5'6'b}$ 3.3 Hz, H-5′), 2.08, 2.04, 2.01, 2.00, 1.98 (5s, 24H, Ac, NHAc). ^{13}C NMR (125.7 MHz, $CDCl_3$), Table 1 and δ 170.3, 170.1, 170.05, 170.0, 169.8, 169.4, 169.1, 168.8 (8CO of Ac and NHAc), 154.9 (C-4 of $C_6H_4OCH_3$), 151.0 (C-1 of $C_6H_4OCH_3$), 138.4–114.3 (16C aromatic), 76.5 (C-3), 76.2 (C-4′), 75.3 (C-4), 74.3 (C-5), 73.3, 72.9 (2 CH_2Ph), 72.7 (C-3″), 72.5 (C-5′), 72.0 (C-3′), 71.8 (C-5″), 71.6 (C-2′), 71.3 (C-2″), 68.5 (C-6), 67.5 (C-4″), 61.6 (C-6′), 61.3 (C-6″), 55.4 ($C_6H_4OCH_3$), 52.8 (C-2), 20.5, 20.4, 20.3 (4 $COCH_3$). FABMS: *m/z* 1125 (4%, M^+) and 1148 [100%, $(M+Na)^+$]. *Anal.* Calc. for $C_{55}H_{67}NO_{24}$: C, 58.67; H, 5.96; N, 1.24. Found: C, 59.31; H, 5.94; N, 1.32.

p-*Methoxyphenyl* O-β-*D-glucopyranosyl-(1→4)-*O-β-*D-glucopyranosyl-(1→4)-2-acetamido-3,6-di-*O-*benzyl-2-deoxy-β-*D-glucopyranoside* **4**

To a solution of **3** (1.80 g, 1.6 mmol) in methanol (60 mL) MeONa in methanol (1 M, 3 mL) was added. The reaction mixture was stirred at r.t. for 2 h, made neutral with Amberlyst IRA-120 (H^+), filtered and evaporated in vacuo. The residue was crystallised from ethanol to give **4** (1.31 g, 99%) as white solid. FABMS: *m/z* 854 [100%, $(M+Na)^+$]. *Anal.* Calc. for $C_{41}H_{53}NO_{17}$: C, 59.21; H, 6.38; N, 1.68. Found: C, 59.28; H, 6.44; N, 1.88.

p-*Methoxyphenyl* O-*(4,6-*O-*benzylidene-*β-*D-glucopyranosyl)-(1→4)-*O-β-*D-glucopyranosyl-(1→4)-2-acetamido-3,6-di-*O-*benzyl-2-deoxy-β-*D-glucopyranoside* **5**

To a solution of **4** (1.31 g, 1.6 mmol) in freshly distilled benzaldehyde (20 mL) $ZnCl_2$ (0.44 g) was added. The reaction mixture was stirred for 16 h at r.t. and then washed with water (3×25 mL). Petroleum ether was added to the organic layer and a white solid was obtained which was filtered off and washed with water, petroleum ether and diethyl ether to give **5** (1.31 g, 90%) as a white solid that recrystallised from ethanol had m.p. 201–203°C; $[\alpha]_D$ +11.8 (*c* 1.1, methanol). FABMS: *m/z* 942 [90%, $(M+Na)^+$]. *Anal.* Calc. for $C_{48}H_{57}NO_{17}$: C, 62.68; H, 6.20; N, 1.52. Found: C, 62.70; H, 6.36; N, 1.55.

p-*Methoxyphenyl* O-*(2,3-di-*O-*acetyl-4,6-*O-*benzylidene-*β-*D-glucopyranosyl)-(1→4)-*O-*(2,3,6-tri-*O-*acetyl-*β-*D-glucopyranosyl)-(1→4)-2-acetamido-3,6-di-*O-*benzyl-2-deoxy-*β-*D-glucopyranoside* **6**

To a solution of **5** (0.02 g, 0.02 mmol) in pyridine (1 mL) acetic anhydride (0.5 mL) was added at 0°C. After 16 h methanol was added at 0°C to destroy the excess of acetic anhydride. The solvents were evaporated in vacuo and by coevaporation with toluene. Compound **6** (0.02 g, 91%) was obtained as an amorphous solid; $[\alpha]_D$ +28.8 (*c* 0.7, dichloromethane). ^1H NMR (500 MHz, $CDCl_3$), Table 1 and δ 7.35–7.20 (m, 15H, Ph), 6.88–6.69 (m, 4H, $C_6H_4OCH_3$), 5.82(d, 1H, $J_{2,NH}$ 8.1 Hz, N*H*), 5.41 (s, 1H, C*H*Ph), 5.23–5.19 (m, 1H, H-3″), 5.03 (t, 1H, $J_{3',4'}$ 9.5 Hz, H-3′), 4.86 (t, 1H, $J_{2'',3''}$ 8.0 Hz, H-2″), 4.80 (t, 1H, $J_{2',3'}$ 9.2 Hz, H-2′), 4.70, 4.58, 4.48, 4.33 (4d, 1H each, $^2J_{H,H}$ 11.8, 11.7, 11.9, 11.9 Hz, CH_2Ph), 4.29–4.25 (m, 1H, H-6″a), 3.97 (dd, 1H, $J_{5',6'a}$ 4.8 Hz, $J_{6'a,6'b}$ 12.1 Hz, H-6′a), 3.94 (t, 1H, $J_{4,5}$ 6.7 Hz, H-4), 3.89 (t, 1H, $J_{3,4}$ 6.7 Hz, H-3), 3.73–3.68 (m, 1H, H-6″b), 3.78 (dd, 1H, $J_{5,6a}$ 4.2 Hz, $J_{6a,6b}$ 10.0 Hz, H-6a), 3.68–3.59 (m, 4H, H-4′, H-4″, H-5, H-6′b), 3.41–3.37 (m, 2H, H-5″, H-6b), 3.68 (s, 3H, OCH_3), 3.27 (ddd, 1H, $J_{4,5}$ 9.5 Hz, $J_{5,6b}$ 2.7 Hz, H-5′), 1.99, 1.96, 1.95, 1.94, 1.94, 1.90, 1.81 (7s, 18H, Ac, NHAc). ^{13}C NMR (75.4 MHz, $CDCl_3$), Table 1 and δ 170.2–169.3 (6C, 5CO of Ac and NHAc), 154.9 (C-4 of $C_6H_4OCH_3$), 151.1 (C-1 of $C_6H_4OCH_3$), 138.4–114.3 (22C aromatic), 101.5 (*C*HPh), 77.8–71.7 (10C, sugar ring carbons), 73.4, 73.0 (2 CH_2Ph), 68.5 (C-6), 68.3 (C″-6), 66.2 (C-4″), 61.7 (C′-6), 55.5 ($C_6H_4OCH_3$), 52.9 (C-2), 20.5, 20.4, 20.3 (6 $COCH_3$). FABMS: *m/z* 1152 [100% $(M+Na)^+$].

p-*Methoxyphenyl* O-*(2,3-di-*O-*benzyl-4,6-*O-*benzylidene-*β-*D-glucopyranosyl)-(1→4)-*O-*(2,3,6-tri-*O-*benzyl-*β-*D-glucopyranosyl)-(1→4)-2-acetamido-3,6-di-*O-*benzyl-2-deoxy-*β-*D-glucopyranoside* **7**

To a solution of **5** (5.00 g, 5.4 mmol) in DMF (26 mL), powdered NaOH (3.27 g, 80.0 mmol) and a solution of $(Bu^t_4N)HSO_4$ (0.21 g, 0.54 mmol) in *t*-butanol (30 mL). The mixture was vigorously

stirred for 15 minutes, and then benzyl bromide (10 mL, 80.0 mmol) was added dropwise. After 16 h with vigorous stirring at r.t., the reaction mixture was diluted with dichloromethane and the unreacted NaOH was filtered off through Celite. The solution was washed with water (3×30 mL), dried ($MgSO_4$) and evaporated to dryness. Column chromatography of the residue on silica gel (toluene–acetone, 20:1→8:1) gave **7** (4.38 g, 60%) as an oil. FABMS: *m/z* 1392 [27%, $(M+Na)^+$].

p-*Methoxyphenyl* O-*(2,3,6-tri-*O*-benzyl-β-D-glucopyranosyl)-(1→4)-*O*-(2,3,6-tri-*O*-benzyl-β-D-glucopyranosyl)-(1→4)-2-acetamido-3,6-di-*O*-benzyl-2-deoxy-β-D-glucopyranoside* **9**

Procedure (a): Dry hydrogen chloride in diethyl ether was added at 0°C to a solution of **7** (2.93 g, 2.1 mmol) and $NaCNBH_3$ (1.35 g, 21.4 mmol) in dry THF (35 mL) containing 4 Å molecular sieves until pH 3–4. After 2 h at 0°C, a t.l.c. analysis (toluene–acetone, 4:1) indicated completed reaction. The reaction mixture was poured into ice–water and extracted with dichloromethane (2×30 mL). The organic layer was washed successively with aq NaCl, aq $NaHCO_3$ and water, dried (Na_2SO_4) and evaporated. Compound **9** (1.61 g, 60%) was obtained as an amorphous white solid $[\alpha]_D$ +9.1 (*c* 0.9, dichloromethane).

Procedure (b): To a solution of **7** (2.34 g, 1.71 mmol) and $TsOH \cdot H_2O$ (34 mg, 0.18 mmol) in methanol-1,4-dioxane (50 mL) was heated at 60°C for 2 h. Then $TsOH \cdot H_2O$ (34 mg, 0.18 mmol) was added and heated at 80°C for another 1.5 h. The reaction mixture was made neutral with Et_3N and evaporated to dryness. Column chromatography of the residue on silica gel (toluene–acetone, 10:1→6:1) gave *p*-methoxyphenyl *O*-(2,3-di-*O*-benzyl-β-D-glucopyranosyl)-(1→4)-*O*-(2,3,6-tri-*O*-benzyl-β-D-glucopyranosyl)-(1→4)-2-acetamido-3,6-di-*O*-benzyl-2-deoxy-β-D-glucopyranoside (1.20 g, 55%) **8**.

A mixture of **8** (0.70 g, 0.55 mmol), Bu_2SnO (0.21 g, 0.85 mmol), Bu_4NBr (0.27 g, 0.88 mmol) and BnBr (0.33 mL, 2.82 mmol) in dry acetonitrile (120 mL) was heated under reflux with a Soxhlet apparatus containing 3 Å molecular sieves for 3 days. The Soxhlet apparatus was removed and Et_3N (5 mL) was added and the solution was heated under reflux for 1 hour to destroy the excess of BnBr and then concentrated to dryness. The residue was dissolved in ethyl acetate (60 mL) and saturated aq $NaHCO_3$ (40 mL) was added. The mixture was stirred vigorously for 3 h filtered and the organic layer washed with saturated aq KCl, dried (Na_2SO_4) and evaporated. The purification was performed by chromatographic column on silica gel (toluene–acetone, 15:1→8:1) to afford **9** (0.60 g, 80%). ^1H NMR (500 MHz, $CDCl_3$), Table 1 and δ 7.35–7.23 (m, 40H, Ph), 6.78–6.98 (m, 4H, $C_6H_4OCH_3$), 5.77 (d, 1H, $J_{2,NH}$ 7.8 Hz, N*H*), 5.01, 4.84 (2d, 1H each, $^2J_{H,H}$ 11.0, 12.1 Hz, CH_2Ph), 4.81–4.33 (m, 14H, CH_2Ph), 4.11 (t, 1H, $J_{2,3}$ 8.1 Hz, $J_{3,4}$ 8.1 Hz, H-3), 4.07–3.80 (m, 3H, H-4, H-4′, H-4″), 3.75–3.71 (m, 1H, H-2), 3.63 (t, 1H, $J_{3',4'}$ 9.0 Hz, H-3′), 3.65–3.20 (m, 6H, H-5′, H-5″, H-6′a, H-6′b, H-6″a, H-6″b), 3.57–3.51 (m, 2H, H-6a, H-6b), 3.48 (t, 1H, 1H, $J_{3'',4''}$ 9.0 Hz, H-3″), 3.41–3.36 (m, 1H, H-2′), 3.36–3.31 (m, 1H, H-2″), 3.26–3.20 (m, 1H, H-5), 3,79 (s, 3H, OCH_3), 1.80 (s, 3H, NHAc). ^{13}C NMR (125.7 MHz, $CDCl_3$), Table 1 and δ 170.2 (CO de NHAc), 155.0 (C-4 of $C_6H_4OCH_3$), 151.3 (C-1 de $C_6H_4OCH_3$), 143.7–114.5 (52C aromatic), 84.2–74,8 (11C, sugar ring carbons), 73.7–72.9 (8C, $8CH_2Ph$), 71.5 (C-6), 68.5, 67.9 (C-6′, C-6″), 55.5 ($C_6H_4OCH_3$), 54.5 (C-2), 23.3 ($COCH_3$). FABMS: *m/z* 1395 [100%, $(M+Na)^+$]. *Anal.* Calc. for $C_{83}H_{89}NO_{17}$: C, 72.65; H, 6.49; N, 1.02. Found: C, 72.53; H, 6.50; N, 1.30.

p-*Methoxyphenyl* O-*(4-*O*-acetyl-2,3,6-tri-*O*-benzyl-β-D-glucopyranosyl)-(1→4)-*O*-(2,3,6-tri-*O*-benzyl-β-D-glucopyranosyl)-(1→4)-2-acetamido-3,6-di-*O*-benzyl-2-deoxy-β-D-glucopyranoside* **10**

To a solution of **9** (15 mg, 0.01 mmol) in pyridine (1 mL) acetic anhydride (0.5 mL) at 0°C was added. The reaction mixture was left at r.t. for 16 h. Methanol at 0°C was added to destroy the excess of acetic anhydride and then concentrated to dryness by coevaporation with toluene. Compound **10** (13 mg, 95%) was obtained as an amorphous white solid, $[\alpha]_D$ +12.0 (*c* 1.0, dichloromethane). ^1H NMR (500 MHz, $CDCl_3$), Table 1 and δ 7.32–7.21 (m, 40H, 8Ph), 6.96–6.76 (m, 4H, $C_6H_4OCH_3$), 5.74 (d, 1H, $J_{2,NH}$ 7.8 Hz, N*H*), 5.01, 4.91, 4.23 (3d, 1H each, $^2J_{H,H}$ 10.9, 12.1, 11.8 Hz, CH_2Ph), 4.81–4.33 (m, 13H, CH_2Ph), 4.96 (t, 1H, $J_{3'',4''}$ 9.0 Hz, $J_{4'',5''}$ 9.0 Hz, H-4″), 4.81–4.33, 4.09–3.36,

3.48–3.39, 3.35–3.19 (4m, sugar ring protons), 3.48–3.39 (m, 2H, H-3″, H-5″), 3.75 (s, 3H, OCH_3), 1.81, 1.80 (2s, 3H each, Ac, NHAc). ^{13}C NMR (75.4 MHz, $CDCl_3$), Table 1 and δ 170.2, 169.6 (2CO of Ac, NHAc), 155.0 (C-4 of $C_6H_4OCH_3$), 151.2 (C-1 of $C_6H_4OCH_3$), 138.9–127.2 (52C aromatic), 82.8–71.4 (11C, sugar ring carbons), 73.7–73.0 (8C, $8CH_2Ph$), 70.0 (C-6), 68.4, 67.8 (C-6′, C-6″), 55.5 ($C_6H_4OCH_3$), 54.9 (C-2), 23.6, 20.3 ($2COCH_3$). FABMS: *m/z* 1438 [100%, $(M+Na)^+$].

p-*Methoxyphenyl* O-*(3,4,6-tri*-O-*acetyl-2-deoxy-2-phthalimido-β-D-glucopyranosyl)-(1→4)-(2,3,6-tri*-O-*benzyl-β-D-glucopyranosyl)-(1→4)*-O-*(2,3,6-tri*-O-*benzyl-β-D-glucopyranosyl)-(1→4)-2-acetamido-3,6-di*-O-*benzyl-2-deoxy-β-D-glucopyranoside* **12**

A mixture of **9** (1.00 g, 0.73 mmol), AgOTf (0.12 g, 0.36 mmol), 4 Å molecular sieves in dry dichloromethane (6 mL), was stirred at r.t. for 30 minutes under argon. A solution of 3,4,6-tri-*O*-acetyl-2-deoxy-2-phthalimido-β-D-glucopyranosyl trichloroacetimidate (**11**) (0.20 g, 0.36 mmol) in dichloromethane (6 mL) under Ar was transferred. The reaction mixture was stirred at r.t. and solutions of AgOTf (0.48 g, 1.44 mmol) in dichloromethane (10 mL) and **11** (0.40 g, 0.72 mmol) in dichloromethane (8 mL) were added in three portions after periods of three hours. The reaction mixture was stirred at r.t. for 40 h, diluted with dichloromethane and filtered. The solution was washed successively with saturated aq $NaHCO_3$ and water, dried (Na_2SO_4) and evaporated to dryness. Column chromatography of the residue over silica gel (ethyl ether petroleum ether 4:1→10:1) gave **12** (0.78 g, 60%) as a white solid, that crystallised from ethanol had m.p. 72–74°C (ethanol); $[\alpha]_D$ +6.0 (*c* 0.7, dichloromethane). ^1H NMR (500 MHz, $CDCl_3$), Table 1 and δ 7.80–6.95 (m, 48H, $8CH_2Ph$, NPhth), 6.95–6.70 (m, 4H, $C_6H_4OCH_3$), 5.73 (d, 1H, $J_{2,NH}$ 7.6 Hz, N*H*), 5.69 (dd, 1H, $J_{2''',3'''}$ 10.7 Hz, H-3‴), 5.11 (t, 1H, $J_{3''',4'''}$ 9.1 Hz, H-4‴), 5.02, 4.99, 4.86, 4.45 (4d, 1H each, $^2J_{H,H}$ 11.8, 11.9, 11.7, 11.9 Hz, CH_2Ph), 4.77–4.58 (m, 7H, CH_2Ph), 4.40–4.16 (m, 14H of the sugar ring, 5H de CH_2Ph), 4.16–4.03 (m, 2H, H-3, H-6a), 3.97 (t, 1H, $J_{3,4}$ 7.3 Hz, $J_{4,5}$ 7.3 Hz, H-4), 3.74–3.67 (m, 2H, H-2, H-5), 3.60–3.50 (m, 1H, H-6b), 3.32–3.24 (m, 1H, H-5‴), 3.10 (m, 1H, H-5″) 3.74 (s, 3H, OCH_3), 1.97, 1.94, 1.83, 1.76 (4s, 3H each, 3Ac, NHAc). ^{13}C NMR (125.7 MHz, $CDCl_3$), Table 1 and δ 170.6 (2C), 170.2, 170.1 (4CO of 3Ac and NHAc), 169.4 (2CO of NPhth), 155.3 (C-4 of $C_6H_4OCH_3$), 149.8 (C-1 of $C_6H_4OCH_3$), 139.1–127.0 (58C, aromatic), 83.0, 82.9, 82.1, 81.8, 76.6, 73.1, 73.4, 73.3, 72.9, 72.3, 71.4, 70.6, 68.5, 68.0, 67.8, 66.5, 64.8, 62.3, 61.3 (19 sugar ring carbons), 75.5, 75.2, 75.0, 74.99, 74.8, 74.7, 74.6, 74.1 ($8CH_2Ph$), 55.5 ($C_6H_4OCH_3$), 55.2, 54.8 (C-2, C-2‴), 20.6, 20.5(2C), 20.3 ($4COCH_3$,). FABMS: *m/z* 1812 [88%, $(M+Na)^+$]. *Anal.* Calc. for $C_{103}H_{108}N_2O_{26}$: C, 69.73; H, 6.04; N, 1.56. Found: C, 68.88; H, 5.99; N, 1.68.

p-*Methoxyphenyl* O-*(2-deoxy-2-phthalimido-β-D-glucopyranosyl)-(1→4)-(2,3,6-tri*-O-*benzyl-β-D-glucopyranosyl)-(1→4)*-O-*(2,3,6-tri*-O-*benzyl-β-D-glucopyranosyl)-(1→4)-2-acetamido-3,6-di*-O-*benzyl-2-deoxy-β-D-glucopyranoside* **13**

To a solution of **12** (0.1 g, 0.06 mmol) in methanol (4 mL) NaMeO/MeOH (1M, 0.5 mL) was added. The reaction mixture was left at r.t. for 2 h, made neutral with Amberlist IRA-120 (H^+), filtered and concentrated to dryness. Crystallisation from ethanol of the residue gave **12** (89 mg, 90%) as a white solid. FABMS: *m/z* 1686 [12%, $(M+Na)^+$]. *Anal.* Calc. for $C_{97}H_{102}N_2O_{23}$: C, 70.00; H, 6.13; N, 1.68. Found: C, 69.92; H, 6.52; N, 1.44.

p-*Methoxyphenyl* O-*{2-deoxy-2-[(11Z)-11-octadecaenoylamido]-β-D-glucopyranosyl}-(1→4)*-O*(β-D-glucopyranosyl)(1→4)*-O-*(β-D-glucopyranosyl)-(1→4)-2-acetamido-2-deoxy-β-D-glucopyranoside (16) and* p-*methoxyphenyl* O-*{3,4,6-tri*-O-*acetyl-2-deoxy-2-[(11Z)-11-octadecaenoylamido]-β-D-glucopyranosyl}-(1→4)-(2,3,6-tri*-O-*acetyl-β-D-glucopyranosyl)-(1→4)*-O-*(2,3,6-tri*-O-*acetyl-β-D-glucopyranosyl)-(1→4)-2-acetamido-3,6-di*-O-*acetyl-2-deoxy-β-D-glucopyranoside* **17**

A mixture of **12** (172 mg, 0.096 mmol) and $Pd(OH)_2$–C (20%, 86 mg) in ethanol–THF (1:1, 100 mL) was hydrogenated at 3 atm and r.t. for 18 h. The mixture was filtered off and the solution concentrated to dryness to give the crude *p*-methoxyphenyl *O*-(3,4,6-tri-*O*-acetyl-2-deoxy-2-phthalimido-β-D-glucopyranosyl)-(1→4)-β-D-glucopyranosyl-(1→4)-*O*-β-D-glucopyranosyl-(1→4)-2-acetamido-2-

deoxy-β-D-glucopyranoside (**14**) {92 mg, FABMS: *m/z* 1091 [25%, $(M+Na)^+$]}. To a solution of the crude **14** (92 mg, 0.086 mmol) in ethanol (15 mL) $N_2H_4 \cdot H_2O$ (0.42 mL, 1.1 mmol) was added. The reaction mixture was heated under reflux for 3 days. Traces of $N_2H_4 \cdot H_2O$ were eliminated by coevaporation with toluene and methanol to give *O*-(2-amino-2-deoxy-β-D-glucopyranosyl)-(1→4)-β-D-glucopyranosyl-(1→4)-*O*-β-D-glucopyranosyl-(1→4)-2-acetamido-2-deoxy-β-D-glucopyranoside **15** as a syrup. A solution of the crude **15** in DMF (3 mL), Et_3N (0.13 mL, 0.98 mmol), 2-chloro-1-methylpiridinium iodide (230 mg, 0.88 mmoles) and vaccenic acid (250 mg, 0.88 mmol) was added. The reaction was stirred at r.t. for 4 h and concentrated to dryness to give **16** (21 mg, 22%) as an amorphous solid; $[\alpha]_D$ −10.0° (*c* 0.7, methanol), NMR data: Table 2. Compound **16** was conventionally acetylated, at 0°C→r.t., with acetic anhydride/pyridine 1:1 (4 mL) for 24 h. Excess of acetic anhydride was destroyed by adding methanol and the solution concentrated to dryness by coevaporating with toluene. Column chromatography of the residue over silica gel (toluene–acetone 8:1→2:1) gave **17** (30 mg, 22%) as an amorphous solid, $[\alpha]_D$ −3.5 (*c* 0.9, dichloromethane). ^1H NMR (500 MHz, $CDCl_3$), Table 1 and δ 6.93–6.79 (m, 4H, $C_6H_4OCH_3$), 5.78, 5.74 (2d, 1H each, $J_{2,NH}$ 8.7, 9.2 Hz, N*H*), 5.37–5.35 (m, 2H, H-9, H-10 chain), 5.23 (t, 1H, $J_{2,3}$ 9.4 Hz, $J_{3,4}$ 9.4 Hz, H-3), 4.87–4.82 (m, 1H, H-4), 5.17–4.82, 4.56–3.45 (2m, sugar ring protons), 3.77 (s, 3H, OCH_3), 2.16, 2.15, 2.14, 2.13, 2.12, 2.09, 2.08, 2.06, 2.05, 2.04, 2.02, 2.01, 2.00, 1.99, 1.97 (s, 38H, 12Ac, 2H lipid chain), 1.33–1.22 (m, 24H, CH_2 lipid chain), 0.91–0.88 (m, 3H, CH_3 lipid chain). ^{13}C NMR (125.7 MHz, $CDCl_3$), Table 1 and δ 173.2 170.8, 170.4(2C), 170.3(2C), 170.2, 170.0, 169.7, 169.6, 169.4, 169.3, 169.2 (13CO of NHAc, Ac), 155.3 (C-4 of $C_6H_4OCH_3$), 150.9 (C-1 of $C_6H_4OCH_3$), 129.8, 129.7, 118.1, 114.4 (4C aromatic), 76.1, 75.5, 73.0, 72.7, 72.64, 72.6, 72.4, 72.05, 71.8, 71.64, 71.6, 71.4, 68.0, 62.2, 61.8, 61.6, 61.5 (18C, sugar ring carbons), 55.5 ($C_6H_4OCH_3$), 54.6, 53.0 (C-2, C-2′), 36.5, 31.6, 29.6, 29.59, 29.4, 29.3, 29.2, 29.23, 29.1, 28.7, 27.1, 25.3, 23.1, 22.5, 20.8, 20.7, 20.5, 20.4, 20.3, 14.0 ($12COCH_3$ and lipid chain carbons). FABMS: *m/z* 1561 [100%, $(M+Na)^+$]. *Anal.* Calc. for $C_{73}H_{106}N_2O_{33}$: C, 56.96; H, 6.89; N, 1.82. Found: C, 57.01; H, 6.89; N, 2.15.

Conformational analysis

MC-search

The calculations were performed in a Silicon Graphics workstation with the MM3* force field as integrated in MACROMODEL[42] v4.5. The MM3* differs from the regular MM3[43] force field in the treatment of the electrostatic term, since it employs charge–charge instead of dipole–dipole interactions. The glycosidic torsion angles of **1** (see Figure 1) φ1, φ2, φ3 were defined as H1′-C1′-O1′-C4 and ψ1, ψ2, ψ3 as H4-C4-O1′-C1′. The hydroxymethyl torsion angles ω1, ω2, ω3 and ω4 were defined as O5-C5-C6-O6.

Four MC-searches were performed using different initial structures. The Glc and GlcN moieties were left in their more stable $^4C_1$ chair conformations. All the glycosidic linkages φ were set close to the exo-anomeric[44] position, since this orientation has been shown to be strongly predominant for similar linkages. Different combinations of the *gg*/*gt* rotamers were chosen for the ω torsion of the hydroxymethyl groups for each pyranoid ring, since both rotamers are populated in solution in glucose-type configurations.[45] The initial structure of each MC was previously minimized in vacuum using MM3* (ε=80) and then submitted to 1000 MC steps. The following torsions were modified during each MC-step: all the φ/ψ torsions, all the hydroxymethyl groups ω, and the three torsions of the lipid chain closest to residue GlcN-4, which were labeled as R1, R2 and R3, respectively. Between 2 and 11 torsions were randomly selected for variation at each MC step. Then, the resultant geometry was minimized using 5000 gradient conjugate steps. Structures were tested for duplication according to a least square criteria. An energy window of 50 $KJ.mol^{-1}$ was used as energy criterion to accept a given conformation. A total of 2120 MC-steps were accepted during the four MC-searches, then processed to remove repeated structures, and, finally, a total of 354 different conformers were obtained. Only three of these minima (Min. 1, Min. 2 and Min. 3) had steric energy values below 12 $KJ.mol^{-1}$ over that corresponding to the global minimum.

In a second step, the conformational space around the global minimum was scanned by generation of fifteen different structures. These conformers were built by using the global minimum as starting geometry, and combining the four hydroxymethyl torsions as either *gg* or *gt* arrangements, then producing fifteen combinations. These conformers were subsequently minimized in vacuum by using MM3* (ϵ=80).

Molecular dynamics

The geometry of the global minimum, Min. 1, previously obtained in the MC simulations was used as starting structure for two independent molecular dynamics simulations (MD), quoted in the text as MD-I and MD-II.

MD-I was performed by using the MM3* force field, and the GB/SA solvent model[36] for water, as implemented in the MACROMODEL package, with a Silicon Graphics INDY computer. The geometry of Min. 1 was extensively minimized in these conditions, and then used as starting point for the MD simulation. The temperature was set constant at 300 K during all the simulation by coupling to a thermal bath. The SHAKE algorithm was used for keeping the C–H bonds fixed. A time step of 1 fs was employed. An equilibration time of 80 ps was used, and trajectory frames were saved at 1 ps intervals during the remaining 500 ps of the simulation, for further analysis.

MD-II was performed in vacuo using the CVFF force field[38] (ϵ=80), as integrated in the INSIGHTII/DISCOVER package, on a Silicon Graphics INDY computer. Min. 1 was extensively minimized in these conditions and then used as starting point for the simulation. The temperature was set constant at 300 K during all the simulation by coupling to a thermal bath. A time step of 1 fs was also employed. The equilibration time was set at 80 ps, and then trajectory frames were saved every ps during the remaining 500 ps of the simulation, for subsequent analysis.These frames of MD-I and MD-II were analyzed using home-made programs, available from the authors upon request.

Acknowledgements

We thank Dr A. Gil-Serrano for helpful discussions, the Dirección General de Investigación Científica y Técnica for Financial support (grant numbers PB94/1440-C02-01 and PB-93-0127) and the Ministerio de Educación y Cultura of Spain for a fellowship to E.L-B.

References

1. a) For a minireview, see Spaink, H. P. *Plant Molecular Biology*, **1992**, *20*, 977–986. b) Promé, J. C.; Demont, N. *Plant -Microb Interaction,* Gary Stacey Ed., Chapman, London, **1996**, pp. 272–309. c) Relic, B.; Talmort, F.; Kopisinka, J.; Gobionowski, W.; Promé, J. C.; Groughton, W. J. *Plant-Microb Interaction,* **1993**, *6*, 764–774. d) Truchet, G.; Roche, P.; Lerouge, P.; Vasse, J.; Camut, S.; de Billy, F.; Promé, J. C.; Denarié, *Nature*, **1991**, *351*, 670–673.
2. a) Lerouge, P.; Roche, P.; Faucher, C.; Truchet, G.; Promé, J. C.; Denarié, J. *Nature*, **1990**, *344*, 781–784. b) Schultze, M.; Quiclet-Sire, B.; Kondorosi, E.; Virelizier, H.; Glunska, J. N.; Endre, G.; Géro, S. D.; Kondorosi, A. *Proc. Natl. Acad. Sci. USA*, **1992**, *89*, 192–196.
3. a) Spaink, H. P.; Shelley, D. M.; van Brussel, A. A. N.; Glushka, J.; York, W. S.; Tak, T.; Geiger, O.; Kennedy, E. P.; Reinhold, V. N.; Lutenberg, B. J. J. *Nature*, **1991**, *354*, 125–130. b) Firmin, J. L.; Wilson, K. E.; Carlson, R. W.; Davies, A. E.; Doronie, J. A. *Mol. Microbiol.* **1993**, *10*, 351–360.
4. a) Sanjuan, J.; Carlson, R. W.; Spaink, H. P.; Bhat, U. R.; Barbour, W. M.; Gluska, J.; Stacey, G. *Proc. Natl. Acad. Sci. USA*, **1992**, *89*, 8789–8793. b) Carlson, R. W.; Sanjuan, J., Bhat, U. R.; Glushka, J.; Spaink, H. P.; Wijfjes, A. H. M.; van Brussel, A. A. N.; Stokermans, T. J. W.; Peters, K.; Stacey, G. *J. Biol. Chem.* **1993**, *268*, 18372–18381.
5. Bec-Ferté, M.-P.; Krishnan, H. B.; Savagnac, A.; Pueppke, S. G.; Promé, J. C. *FEBS Letters* **1996**, *393*, 273–279.
6. Nicolaou, K. C.; Bockovich, N. J.; Carcanague, D. R.; Hummel, C. W.; Even, L. F. *J. Am. Chem. Soc.*, **1992**, *114*, 8701–8702.

7. Wang, L. X.; Li, C.; Wang, Q. W.; Hui, Y. Z. *Tetrahedron Letters*, **1993**, *34*, 7763–7766; and *J. Chem. Soc. Perkin Trans. I*, **1994**, 621–628.
8. Ikeshita, S.; Nakahara, Y.; Ogawa, T. *Glycoconjugate J.* **1994**, *11*, 257–261.
9. Ikeshita, S.; Sakamoto, A.; Nakahara, Yu.; Nakahara, Yo.; Ogawa, T. *Tetrahedron Letters*, **1994**, *35*, 3123–3126.
10. Tailler, D.; Jacquinet, J. C.; Beau, J. M. *J. Chem. Soc. Chem. Commun.* **1994**, 1827–1828.
11. Robina, I.; López-Barba, E.; Fuentes, J. *Tetrahedron*, **1996**, *52*, 10771–10784.
12. Auzanneau, F.-I.; Fanton, E.; Defaye, J.; Gelas, G.; Presented at the XVIII International Carbohydrate Symposium, Milan, Italy, July **1996**. Book of Abstracts, Abstr. BP062. p. 319.
13. Van Leeuwen, S. H.; van der Marel, G. A.; Spaink, H. P.; Lugtenberg, B. J. J.; van Boom, J. H. Same Symposium of reference 12. Book of Abstracts, Abstr. B.P. 158 p. 413.
14. Zinin, A.; Malysheva, N. N.; Shaskov, S.; Shivaev, V. N.; Torgov, V. I.; Broughton, W. J. Same Symposium of reference 12. Book of Abstracts, Abstr. B.P. 212 p. 467.
15. For a review, see Lockhoff, O. *Angew. Chem. Int. Ed. Eng.* **1991**, *30*, 1611–1620.
16. Devlin, J. P.; Hargrave, K. D. *Tetrahedron*, **1989**, *45*, 4327–4369.
17. a) Avalos, M.; Babiano, R.; Durán, C. J.; Jiménez, J. L.; Palacios, J. C. *J. Chem. Soc. Perkin Trans 2*, **1992**, 2205–2215. b) Ortiz-Mellet, M. C.; Moreno Marín, A.; García-Fernández, J. M.; Fuentes, J.; Moreno Marín, A.; García-Fernández, J. M.; Fuentes, J. *Tetrahedron: Asymmetry*, **1994**, *5*, 2313–2324.
18. Fowler, P.; Bernet, B.; Vasella, A. *Helv. Chim. Acta*, **1996**, *79*, 269–287.
19. Toshima, K.; Tatsuta, K. *Chem. Rev.*, **1993**, *93*, 1503–1531.
20. Robina, I.; López-Barba, E.; Fuentes, J. *Synthetic Commun.*, **1996**, *26*, 2847–2856.
21. Lemieux, R. U.; Abbas, S. Z.; Ching, B. Y. *Can. J. Chem.*, **1984**, *60*, 275.
22. Silwanis, B. A.; El-Sokkary, R. I.; Nashed, M. A. Paulsen, J. *J. Carbohydr. Chem.*, **1991**, *10*, 1067–1078.
23. Lafont, D.; Boullanger, P.; Fenet, B. *J. Carbohydr. Chem.*, **1994**, *13*, 565–583.
24. Schmidt, R. R. *Pure and Appl. Chem.*, **1989**, *61*, 1257–1270.
25. Banoub, J.; Boullanger, P.; Lafont, D. *Chem. Rev.*, **1992**, *92*, 1167–1195.
26. Pumes, B. *J. Am. Chem. Soc.*, **1929**, *9*, 3619–3621.
27. Veeneman, G. H.; van Leeuwen, S. H.; van Boom, J. H. *Tetrahedron Lett.*, **1990**, *31*, 1331–1134.
28. Fuentes Mota, J.; Fernández-Bolaños Guzmán, J. M.; García-Fernández, J. M.; Moreda, W.; Ortiz, C.; Pradera, M. A.; Robina, I.; Welsh, C. *Carbohydr. Res.*, **1992**, *232*, 47–57.
29. Schmidt, R. *Angew. Chem. Int. Ed. Engl.*, **1986**, *25*, 212–235.
30. Grundler, G.; Schmidt, R. *Carbohydr. Res.*, **1985**, *135*, 203–218.
31. Douglas, S. P.; Whitfield, D. M.; Keprinsky, J. J. *J. Carbohydr. Chem.*, **1993**, *12*, 131–136.
32. Sutherland, J. K.; Widdowson, P. A. *J. Chem. Soc.*, **1964**, 650–654.
33. For **3–10** the *p*-methoxyglucosyloxy ring is named ring A. The next two glucosyloxy rings are named as ring B (their nuclei are indicated as H′ and C′) and C (H″ and C″). For **12**, **16** and **17** ring A, B and C are the same as in **3–10** and ring D (H‴ and C‴) is the amino or amido-sugar ring.
34. Stewart, W. E.; Sidall III, T. H. *Chem. Rev.*, **1970**, *70*, 517–551.
35. a) Asensio J. L.; Jiménez-Barbero, J. *Biopolymers*, **1995**, *35*, 55–73. b) Asensio, J. L.; Martín-Pastor, M.; Jiménez-Barbero, J. *J. Biol. Macromol.*, **1995**, *17*, 137–148. c) Hirotsu, K.; Shamada, A. *Bull. Chem. Soc. Jpn.*, **1974**, *47*, 1872–1879.
36. Still, W. C.; Tempczyk, A.; Hawley, R. C.; Hendrickson, T.; *J. Am. Chem. Soc.*, **1990**, *112*, 6127–6129.
37. French, A. D.; Brady, J. W., Eds, *Computer Modeling Carbohydrs Molecules ACS*, **1990**, 430.
38. Hagler, A. T.; Lifson, P.; Dauber, P. *J. Am. Chem. Soc.*, **1979**, *101*, 5122–5130.
39. a) Homans, S. W., *Prog. NMR. Spectrosc.*, **1990**, *22*, 55–86. b) Bock, K. *Pure Appl. Chem.*, **1983**, *55*, 605–622. c) Peters, T.; Meyer, B.; Stuike-Prill, R.; Somorjai, R.; Brisson, J.-R. *Carbohydr. Res.*, **1993**, *238*, 49–73. d) van Halbeek, H. *Curr. Opin. Struct. Biol.*, **1994**, *4*, 697–709. e) Bush,

C. A. *Curr. Opin. Struct. Biol.*, **1992**, *2*, 655–663. f) de Waard, P.; Leeflang, B. R.; Vliegenthart, J. F. G.; Boelens, R.; Vuister, G.; Kaptein, R. *J. Biomol. NMR*, **1992**, *2*, 211–226. j) Rutherford, T. J.; Neville, D. C. A.; Homans, S. W. *Biochemistry*, **1995**, *34*, 14131–14137.

40. Neuhaus, D.; Williamson, M. P. *The Nuclear Overhauser Effect in Structural Conformational Analysis*, **1989**, VCH Publishers, NY.
41. a) Hricovini, M.; Shah, R. N.; Carver, J. P. *Biochemistry*, **1992**, *31*, 10018–10023. b) Rutherford, T. J.; Partridge, J.; Weller, C. T.; Homans, S. W. *Biochemistry*, **1993**, *32*, 12715–12724. c) Hricovini M.; Torri, G. *Carbohydr. Res.*, **1995**, *268*, 59–175. d) Hardy, B. J.; Egan, W.; Widmalm, G. *Int. J. Biol. Macromol.*, **1995**, *17–18*, 149–160. e) Hajduk, P. J.; Horita, D. A.; Lerner, L. *J. Am. Chem. Soc.*, **1993**, *115*, 9196–9201.
42. Mohamadi, F.; Richards, N. G. J.; Guida, W. C.; Liskamp, R.; Caufield, C.; Chang, G.; Hendrickson, T.; Still, W. C. *J. Comput. Chem.* **1990**, *11*, 440–467.
43. Allinger, N. L.; Yuh, Y. H.; Lii, J. H. *J. Am. Chem. Soc.* **1989**, *111*, 8551.
44. a) Lemieux, R. U.; Koto, S. *Tetrahedron*, **1974**, *30*, 1933–1944. b) Kirby, J. A. *The anomeric effect and related stereoelectronic effects at oxygen*, New York, Spinger Verlag, **1983**. c) Tvaroska, I.; Bleha, T. *Adv. Carbohydr. Chem. Biochem.*, **1989**, *47*, 45–123.
45. Bock, K.; Duus, J. O. *J. Carbohydr. Chem.*, **1994**, *13*, 513–543.

(Received in UK 28 January 1997; accepted 4 March 1997)